Recognizing mild cognitive impairment based on network connectivity analysis of resting EEG with zero reference

2014 Physiol. Meas. 35 1279

(http://iopscience.iop.org/0967-3334/35/7/1279)

IOP Publishing | Institute of Physics and Engineering in Medicine Physiological Measurement

Physiol. Meas. 35 (2014) 1279–1298 doi:10.1088/0967-3334/35/7/1279

Recognizing mild cognitive impairment based on network connectivity analysis of resting EEG with zero reference

Peng Xu[1,6,7], **Xiu Chun Xiong**[1,7], **Qing Xue**[2,3,7], **Yin Tian**[1,4], **Yueheng Peng**[5], **Rui Zhang**[1], **Pei Yang Li**[1], **Yu Ping Wang**[2,3,6] **and De Zhong Yao**[1,6]

[1] Key Laboratory for NeuroInformation of Ministry of Education, School of Life Science and Technology, University of Electronic Science and Technology of China, Chengdu 610054, People's Republic of China

[2] Department of Neurology, Xuanwu Hospital, Capital Medical University, Beijing 100053, People's Republic of China

[3] Beijing Key Laboratory of Neuromodulation, Beijing 100053, People's Republic of China

[4] College of Bio-information, ChongQing University of Posts and Telecommunications, Chongqing 400065, People's Republic of China

[5] School of Microelectronics and Solid-State Electronics Physiology, University of Electronic Science and Technology of China, Chengdu 610054, People's Republic of China

E-mail: xupeng@uestc.edu.cn, dyao@uestc.edu.cn and mdwangyp@yahoo.com.cn

Received 27 September 2013, revised 14 February 2014
Accepted for publication 4 April 2014
Published 22 May 2014

Abstract

The diagnosis of mild cognitive impairment (MCI) is very helpful for early therapeutic interventions of Alzheimer's disease (AD). MCI has been proven to be correlated with disorders in multiple brain areas. In this paper, we used information from resting brain networks at different EEG frequency bands to reliably recognize MCI. Because EEG network analysis is influenced by the reference that is used, we also evaluate the effect of the reference choices on the resting scalp EEG network-based MCI differentiation. The conducted study reveals two aspects: (1) the network-based MCI differentiation is superior to the previously reported classification that uses coherence in the EEG; and (2) the used EEG reference influences the differentiation performance, and the zero approximation technique (reference electrode standardization technique, REST) can construct a more accurate scalp EEG network, which results in a higher differentiation accuracy for MCI. This study indicates that the resting

[6] Authors to whom any correspondence should be addressed.

[7] The first three authors have contributed equally to this work.

scalp EEG-based network analysis could be valuable for MCI recognition in the future.

Keywords: mild cognitive impairment, resting scalp EEG, brain network, EEG reference, MCI recognition, zero reference

(Some figures may appear in colour only in the online journal)

1. Introduction

Alzheimer's disease (AD) is the most prevalent neuropathological form that leads to dementia; it affects approximately 25 million people worldwide, and the number of cases is expected to quickly increase in the near future (Babiloni *et al* 2006, Bai *et al* 2012, Fan *et al* 2008, Ferri *et al* 2005, Rossini *et al* 2008, Brookmeyer *et al* 2007, Dauwels *et al* 2010a, Jeong 2004). Mild cognitive impairment (MCI) is characterized by objective evidence of memory impairment that does not yet encompass the definition of dementia (Petersen *et al* 1995, Petrosian *et al* 2001). MCI is often a prodromal stage of AD and is a good target for early diagnosis and therapeutic interventions of AD. Studies show that individuals with MCI tend to progress into AD at a higher rate, approximately 10% to 15% per year (Grundman *et al* 2004, Misra *et al* 2009), compared with healthy controls, who develop dementia at a rate of 1% to 2% per year (Bischkopf *et al* 2002). To provide optimal therapeutic, organizational, and rehabilitative interventions, it would be extremely important to make an early diagnosis of amnesic MCI in normal elderly subjects who are at risk of developing AD (Albert *et al* 2011, Fan *et al* 2008, Misra *et al* 2009, Rossini *et al* 2008, Wee *et al* 2012).

However, MCI is difficult to diagnose due to the very mild symptoms of cognitive impairment and the underlying mechanisms are still unknown (Albert *et al* 2011). Various techniques, including EEG, MEG and fMRI, have been used to study MCI mechanisms. Studies based on EEG and MEG have revealed that MCI subjects displayed a significant decrease in alpha power, a slowing of the EEG, a reduced complexity of the EEG signals, and perturbations in the EEG synchrony compared to normal elderly people (Babiloni *et al* 2006, Koenig *et al* 2005, Rossini *et al* 2008, Dauwels *et al* 2010a, 2011, Jeong 2004). Furthermore, it has been reported that there is a prominent decrease in the functional coupling of EEG rhythms in AD and MCI compared to normal elderly subjects (Adler *et al* 2003, Bai *et al* 2009, Cichocki *et al* 2005, Gomez *et al* 2009, Koenig *et al* 2005, Pijnenburg *et al* 2004, Dauwels *et al* 2010b). MRI-related techniques have been used to study MCI from both structural and functional brain networks (Bai *et al* 2009, 2012, Fan *et al* 2008, Misra *et al* 2009). Clinical patients with MCI showed decreased medial temporal lobe (MTL) activation during a memory encoding task (Dickerson *et al* 2004), and a structural MRI revealed that in addition to gray matter in the hippocampus and the MTL, a number of other regions have displayed significant atrophy, including the orbitofrontal and medial-prefrontal area, cingulate (mainly posterior), insula, uncus, and temporal lobe white matter (Fan *et al* 2008).

The above features, which appear in various imaging techniques, have been attempted for MCI recognition. With respect to EEG-based classification, features such as the global field power, spectral coherence (Coh) and wavelet information have been used as an input, which can achieve approximately 80% accuracy (Acc) (Bennys *et al* 2001, Buscema *et al* 2007, Cichocki *et al* 2005, Rossini *et al* 2008, Stam *et al* 2003). Compared with EEG-based MCI recognition, recognition that is based on MRI imaging can achieve a higher classification Acc (Fan *et al* 2008, Misra *et al* 2009); for example, 96.3% was reported when combined structural and functional MRI features were considered (Wee *et al* 2012).

In essence, the disorder of MCI is closely correlated with abnormal activity in multiple brain areas, as evidenced from fMRI (Bai *et al* 2012, Fan *et al* 2008, Misra *et al* 2009, Wee *et al* 2012); thus, the current brain network approach is more suitable for both interpreting the related mechanisms and performing the MCI recognition. In fact, most of the MRI-related studies are based on structure or functional network analysis to reveal MCI issues such as neural mechanisms and recognition. However, most of the existing EEG-related studies are based on traditional EEG analysis, such as power spectrum and Coh. Compared with the analysis based on MRI, EEG analysis is prone to be affected by the non-zero reference choice (Nunez *et al* 1999, Stam *et al* 2003, Yao 2001) and distorted by the skull, which could be the main reasons why EEG studies on MCI from the perspective of the network are still limited.

The existing studies have proved that the choice of EEG reference greatly influences not only the conventional analyses, such as waveform, power spectrum, and Coh, but also the brain network topology (Marzetti *et al* 2007, Nunez *et al* 1999, Qin *et al* 2010, Yao *et al* 2005, Thatcher 2012). In EEG scalp recordings, only the potential differences between two points can be measured (Geselowitz 1998). However, due to the lack of a neutral (or zero) point on the body surface or insufficient coverage of the head surface by the electrodes, all of those conventional references, such as the vertex reference (VR) and average reference (AR), could inevitably introduce an undesired and unknown temporal bias into the scalp EEG recordings. To entirely resolve the problems that are involved in using body surface points for referencing, a reference with a neutral potential is required. Theoretically, a point at infinity is far from the brain sources and has an ideally zero and neutral potential. Therefore, a point at infinity constitutes an ideal reference (infinity reference, IR) that has a zero or neutral potential. Yao proposed a reference electrode standardization technique (REST) to mathematically re-reference the EEG recordings to IR (Yao 2001). In the present work, REST is adopted to provide reference independent EEG recordings for further network analysis.

As mentioned above, MCI disorder involves multiple brain areas (Bai *et al* 2009, 2012, Fan *et al* 2008, Huang *et al* 2000, Misra *et al* 2009); therefore, network analysis may be a more appropriate approach for studying the related neural mechanisms and the recognition of MCI (Rombouts *et al* 2005, Seo *et al* 2013, Ding *et al* 2013). Moreover, because EEG recording systems are relatively inexpensive and potentially mobile, EEG is equipped in most hospitals and appears to be an attractive brain imaging modality for diagnosing both AD and MCI (Dauwels *et al* 2010a). In the current work, we comparatively constructed the EEG network and performed MCI recognition based on the network properties that are derived from the conventional AR, VR and new IR (REST). Our aim was to improve the possible MCI recognition Acc based on the network mechanisms that underlie MCI and to evaluate the possible reference effect on the differentiation.

2. Materials and methods

2.1. MCI dataset

2.1.1. Subjects. A total of 11 subjects of amnestic MCI (aMCI) were recruited from the Neurological Department of Xuanwu Hospital, and 14 volunteers of normal cognition (NC) from the same community served as the controls in 2011. All of the experimental protocols were approved by the Ethics Committee of Xuanwu Hospital of Capital Medical University, Beijing. Informed consent was obtained from each participant, according to the Declaration of Helsinki.

The aMCI patients satisfied Petersen's revised aMCI criteria. This diagnosis was confirmed using the following inclusion criteria: (i) subjective memory complaint; (ii)

Table 1. Demographic and clinical characteristics of normal controls and aMCIs.

	Control group ($N = 14$)	aMCI group ($N = 11$)	p-value
Mean age, years (± SD)[a]	74.04 ± 6.85	75.50 ± 7.39	0.61
Sex (male: female)[b]	6:8	6:5	0.69
Education, years (± SD)[a]	7.54 ± 3.89	7.05 ± 4.29	0.77
MMSE score (± SD)[a]	26.78 ± 3.72	24.00 ± 5.42	0.14
MoCA score (± SD)[a]	22.36 ± 4.50	16.00 ± 5.08	0.003*
CDR score (IQR)[c]	0.0(0.0–0.0)	0.5(0.5–0.5)	0.000*

[a] Independent-samples *t*-test.
[b] Fisher' s exact test.
[c] Mann–Whitney U test.
MMSE: mini-mental status examination, MoCA: montreal cognitive assessment, CDR: clinical dementia rating scale.

essentially preserved general cognitive function; (iii) objective memory impairment as evidenced by performance of more than 1.5 standard deviations (SDs) below age and education-matched controls for a test called the Chinese Verbal Learning Test; (iv) absence of or very mild impact of impairment in the basic activities of daily life, as determined by a clinical dementia rating (CDR) score of 0.5; a score not greater than 18 on the basic personal activities of daily living (ADL) scale; and (v) absence of dementia according to the DSM-IV criteria.

The inclusion criteria for the NC group were as follows: (i) absence of a subjective memory complaint; (ii) preserved general cognitive function; (iii) performance at 1.5 SD or above age- and education-matched controls for a test, namely, the Chinese Verbal Learning Test; and (iv) absence of impairment in basic activities of daily life, as determined by a CDR score of 0; and a score not greater than 14 on the basic personal ADL scale.

The common inclusion criteria for both groups included being over 60 years of age, living in the same community, and being fluent in hearing and speaking Chinese. The exclusion criteria were as follows: (i) severe vision or hearing impairments that could affect the test processing; (ii) current or previous uncontrolled complicated systemic diseases or head trauma; (iii) history of psychiatric or neurologic disorders, mental retardation, or epilepsy; (iv) alcohol or drug abuse, use of psychoactive drugs, including acetylcholinesterase inhibitors, or taking any tranquilizer, such as benzodiazepine; (v) any focal sign of significant neuropathology, history of cerebral infarction or transient ischemic attack with a Hachinski score of equal to or greater than 4; and (vi) presence of acute anxiety or depression.

The subjects underwent neurological, psychiatric, and neuroimaging examinations, neuropsychological assessment and laboratory testing to ensure that the subjects were free of primary cognitive deficits that result from psychic (e.g., anxiety, depression) or physical (e.g., hypothyroidism, vitamin B12 and folate deficiency, uncontrolled heart disease, uncontrolled diabetes, syphilis) conditions. Neuroimaging examinations included MRI. Moreover, neuropsychological assessment included the mini-mental state examination of Chinese Edition, Montreal cognitive assessment (MoCA) of Chinese Edition, CDR, self-anxiety scale, geriatric depression scale (GDepressionS), global deterioration scale (GDeteriorationS), ADL, and the Hachinski scale. The detailed information for the two groups is listed in table 1.

2.1.2. EEG recordings. The EEG activity was recorded continuously from 60 sites using electrodes that were set in an elastic cap (Greentek, Wuhan, China) and positioned according to the 10–20 International system, including the references, ground, ECG and electrooculogram (EOG). The reference is at the CPz site between Cz and Pz, and the ground electrode was placed in front of the Fpz site. Horizontal and vertical eye movements were detected by recording the EOG, with the use of an additional two electrodes placed 1 cm below (left-hand side) and above (right-hand side) the external canthus. Data were recorded with a band-pass filter of 0.5–70 Hz, a notch of 50 Hz and a digitized data sampling rate of 1024 Hz (Yunshen, Beijing, China). The electrode-skin impedance was set below 5 kΩ. All of the recordings were obtained in the morning with the subjects resting comfortably. An operator will use online camera to monitor the subject's state. If the subject is observed with signs of drowsiness like unconscious nod, the operator will use speaker to alert the subjects and the EEG recording will be stopped to provide enough time for subject to adjust his state. And the new recording procedure will be restarted to record the new EEG until the subject is reported to be ready to perform the experiment awake. Each recording lasted approximately 20 min, with the subject's eyes closed.

2.2. Data preprocessing and re-referencing

All of the recordings were further offline band-pass filtered within 4–40 Hz. Linear detrending and artifact rejection were performed to discard epochs that were contaminated by eye blinks, eye movement, or muscle potentials. The ocular artifacts were defined as EEGs that have amplitude exceeding a $\pm 60\ \mu$v threshold, and muscle movement artifacts were those samples that had characterized high frequency waveforms. EEG data were further visually inspected by two expert electroencephalographists to ensure that the data were free of EOG and muscle movement artifacts.

After the above pre-processing, the EEG recordings of one MCI patient and four controls were observed to be contaminated with obvious artifacts due to the loose contact of the electrodes, and were excluded from further analysis. For each subject in the two groups, ten segments with each approximately 2 s long and free of artifacts were visually selected for further analysis. After above pre-processing, based on the original CPz reference, the recordings were offline re-referenced to AR and IR according to the REST method described by Yao *et al* (2001). In this paper, although the original reference CPz is not the actual vertex at Cz in practice, for convenience in describing the approach, we still use the VR to denote this reference.

2.2.1. Reference electrode standardization technique. REST is a novel method that connects the body reference and the theoretical neural reference at an infinite point. For IR, the forward EEG calculation is (Qin *et al* 2010, Yao 2001)

$$V = GS + e \tag{1}$$

where G is the transfer matrix that is referenced at infinity, which depends on the head model, the source configuration and the electrode montage. V is the vector of potentials that are linearly generated by the source S; and e is the noise. For the vertex referenced recordings V_{VR}, we similarly have

$$V_{\mathrm{VR}} = G_{\mathrm{VR}} S + e \tag{2}$$

where G_{VR} is the EEG lead-field matrix of the VR and V_{VR} is an $M \times N$ matrix of the EEG scalp recording, with M and N being the channel number and sampling points, respectively. The minimum norm solution based on the Moore–Penrose generalized inverse for the source strength S is

$$S = G_{\mathrm{VR}}^{+} V_{\mathrm{VR}} \tag{3}$$

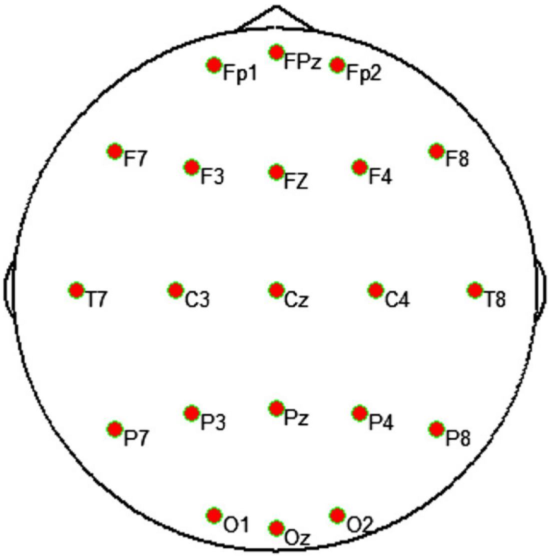

Figure 1. The montage of the selected 21 electrodes from the 10–20 system for network analysis.

where $(\ )^{+}$ denotes the Moore–Penrose generalized inverse and the truncation is used in the Moore–Penrose generalized inverse to address the noise (Qin *et al* 2010, Xu *et al* 2007, 2010b). From the equations, we can see that the source S is the same in the above two equations (1) and (2), which reflects the fact that the reference does not influence the localization and activity of the neural sources. Thus, the IR potential can be reconstructed as the following:

$$V_{\mathrm{IR}} = G(G_{\mathrm{VR}}^{+}V_{\mathrm{VR}}),\ U = GG_{\mathrm{VR}}^{+} \tag{4}$$

where U is the final transfer matrix that is determined by the lead-field matrix G and G_{VR}, both of which are known in advance. Based on the above equations, we can transform the EEGs into genuine EEGs with IR. In the current work, the head model for the REST transformation is a three-concentric-sphere model, the normalized radii of the three concentric spheres are 0.87 (inner radius of the skull), 0.92 (outer radius of the skull) and 1.0 (radius of the scalp), and the conductivities are 1.0, 1.0 and $1/80$ for the brain, scalp and skull; the truncation value that is used for the noise is 0.05. Details of the REST technique, could refer to (Qin *et al* 2010, Yao 2001), and the free software can be downloaded at www.neuro.uestc.edu.cn.

2.2.2. Average reference. Based on the *Vertex* referenced recordings V_{VR}, the EEG recordings V_{AR} with AR were obtained by subtracting the mean voltage waveform calculated across all channels from each individual channel waveform.

2.3. Brain network construction

The brain network can be used to describe the connectivity among multiple regions. For EEG-based network analysis, influence from the volume conduction is inevitable (Marzetti *et al* 2007, Nunez *et al* 1999, Stam *et al* 2003). In this work, 21 canonical electrodes of a 10–20 system were selected from 60 electrodes to construct the brain network (Qin *et al* 2010), aiming to lower the volume conduction effect. Figure 1 shows the montage of the selected 21 electrodes.

2.3.1. Coherence. Coh is the most common way of analyzing the cooperative, synchrony-defined cortical neuronal assemblies, and it represents the linear relationship at a specific frequency between two signals $x(t)$ and $y(t)$ based on their cross-spectrum. In the current work, we adopted the frequency-specific Coh to denote the linkage strength between two network nodes. Coh is expressed as follows (Koopmans 1995):

$$C_{XY}(f) = \frac{|P_{XY}(f)|^2}{P_{XX}(f)P_{YY}(f)} \tag{5}$$

where $P_{XY}(f)$ is the cross-spectrum of $x(t)$ and $y(t)$ at the frequency f, and $P_{xx}(f)$, $P_{yy}(f)$ are the auto spectrum at frequency f estimated from the FFT transformation. Based on the frequency-dependent Coh $C_{XY}(f)$, the edge linkages in the relevant frequency bands, including theta (4–8 Hz), alpha (8–13 Hz), beta (13–30 Hz), gamma (30–40 Hz), and the full band (4–60 Hz), were estimated by averaging the Coh strength within the relevant frequency band.

2.3.2. Network properties. The brain network was constructed based on the Cohs of the 21 nodes, using the corresponding Coh as the edge linkage c_{ij} between two nodes i and j. After constructing the weighted network, the clustering coefficients and shortest path length were used to measure the local and global information processing ability of the brain, respectively. The (weighted) clustering index of vertex i is defined as (Stam *et al* 2009)

$$C_i = \frac{\sum_{k\neq i}\sum_{\substack{l\neq i\\ l\neq k}} c_{ik}c_{il}c_{kl}}{\sum_{k\neq i}\sum_{\substack{l\neq i\\ l\neq k}} c_{ik}c_{il}} \tag{6}$$

where c_{ij} is the edge linkage strength between vertices i and j, which is obtained using equation (5). Then, the mean clustering coefficient (C) of the entire weighted network is determined using (7), as follows:

$$C = \frac{1}{N}\sum_{i=1}^{N} C_i. \tag{7}$$

For the weighted network, the length of the edge between vertices i and j is the inverse of the aforementioned edge weight (Stam *et al* 2009)

$$L_{ij} = \begin{cases} 1/c_{ij}, \text{if} & c_{ij} \neq 0 \\ 1, \text{if} & c_{ij} = 0 \end{cases} . \tag{8}$$

Therefore, the length of a weighted path between two vertices is then defined as the sum of the lengths of the edges of that path. Similarly, the average weighted path length of the entire graph (L) is computed as

$$L = \frac{1}{(1/N(N-1))\sum_{i=1}^{N}\sum_{j\neq i}^{N}(1/L_{ij})}. \tag{9}$$

2.4. Network analysis for the MCI dataset

The above network analysis procedure was performed for each of the 2 s long segments of one subject, which resulted in ten connectivity matrices for each subject. The ten connectivity matrices were further averaged to achieve the final connectivity matrix for analysis. Based on the averaged connectivity matrix, the network topology and properties were calculated for each subject. The two-sample t-test was performed to evaluate the difference in the network properties (clustering coefficients and shortest path length) and the network topology between the groups.

2.5. MCI recognition

The two network properties at different frequency bands were treated as potential inputs for MCI recognition. The receiver operation curve (ROC) was used to evaluate the discriminative ability of those features for MCI recognition. Based on the ROC curves, the features that had a better ROC performance, i.e., a larger area under the curve (AUC), were selected to serve as the final features for MCI recognition. Moreover, to compare the performance of the network-based recognition, the mean coherence (MCoh) of the scalp sensors was also used for MCI recognition (Gomez *et al* 2009). In the current work, linear discrimination analysis (LDA) and support vector machine (SVM) were used to perform the MCI recognition. SVM classification is implemented with the toolbox libsvm using the RBF kernel with default SVM parameter setups (Chang and Lin 2011). To evaluate the classification performance, the Acc, sensitivity (Sen) and specificity (Spe) were used, and the detailed calculations for the three metrics are as follows:

$$\mathrm{Acc} = \frac{n_c + n_{\mathrm{mci}}}{N_c + N_{\mathrm{mci}}} \times 100\%, \quad \mathrm{Sen} = \frac{n_{\mathrm{mci}}}{N_{\mathrm{mci}}} \times 100\%, \quad \mathrm{Spe} = \frac{n_c}{N_c} \times 100\% \tag{10}$$

where N_c and N_{mci} are the actual numbers for the control and MCI patients and n_c and n_{mci} are the correctly predicted numbers for the control and MCI patients.

3. Results

3.1. Topology of the EEG networks

Figure 2 shows the constructed networks for the three references (IR, VR, AR) at different EEG bands, where the network topology is averaged across the subjects for the NC and MCI groups, respectively. Moreover, the two-sample *t*-test was used to compare the topology differences that exist between the two groups, and the edges that had significant differences ($p < 0.05$, Bonferroni correction) between NC and MCI were marked as the difference network (MCI-NC); the red and green edges in figure 2 denote the statistically increased and decreased linkages, respectively. The different network topologies can be observed when the three different references are used (Qin *et al* 2010).

3.2. Network parameters

Figure 3 shows the clustering coefficients and shortest path lengths corresponding to different EEG bands when the three different referencing methods (VR, AR, IR) were used. One-way ANOVA with reference (IR versus AR versus VR) was used to test the network properties on the different oscillatory-band networks, respectively. On the theta network, significant effects of the referencing methods on the cluster coefficient (F (2, 36) = 6.185, $p < 0.005$) and the shortest path length (F (2, 36) = 7.150, $p < 0.003$) were observed, respectively. The interactions between the Ref *group were non-significant (all ps > 0.1). Post hoc *t*-tests (Bonferroni correction) revealed that significant differences on the referencing methods occurred only between AR and VR ($p < 0.004$ on the cluster coefficient; $p<0.003$ on the shortest path length). On the alpha1 network, significant effects of the referencing methods on the cluster coefficient (F (2, 36) = 7.601, $p < 0.004$) and the shortest path length (F (2, 36) = 5.033, $p < 0.012$) were observed. The interaction between the Ref *group was also significant (F (2, 36) = 3.435, $p < 0.044$). Post hoc *t*-tests (Bonferroni correction) revealed that the IR has a significant difference with both AR ($p < 0.006$) and VR ($p < 0.049$) on the cluster coefficient. A significant difference between IR and AR on the shortest path length was also observed ($p < 0.015$). Additionally, a significant effect between the groups (MCI versus normal)

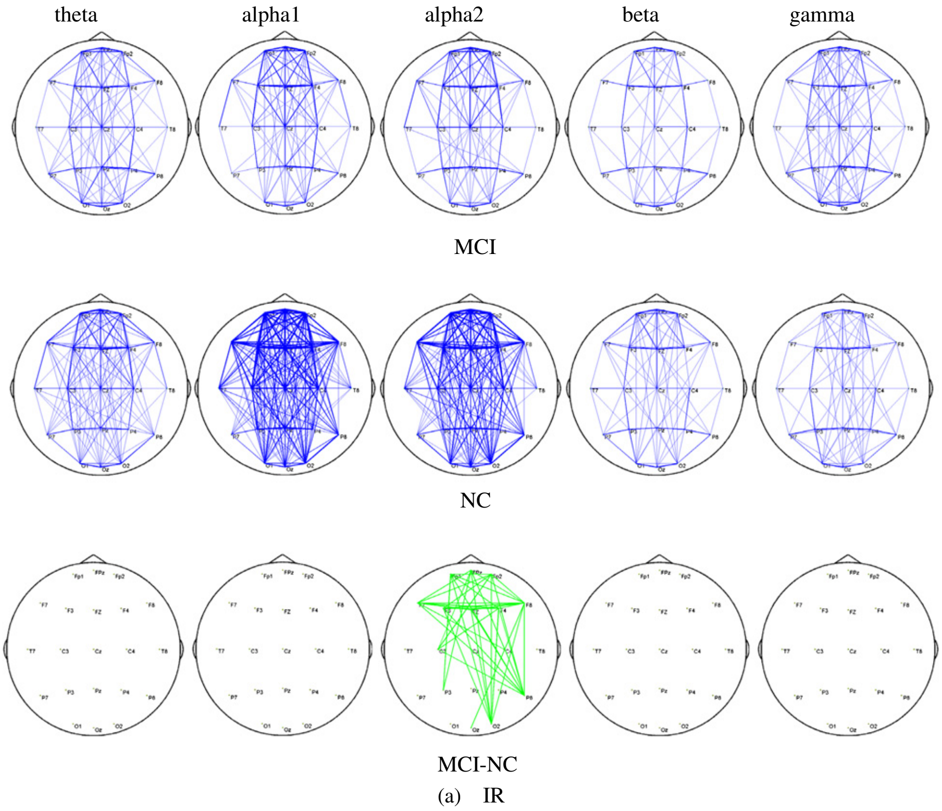

Figure 2. The network topology for different references. Subfigures (a)–(c) correspond to the zero reference (IR), vertex reference (VR) and average reference (AR), respectively. The first and second rows in each subfigure are the corresponding network topology for the MCI and NC; the third row is the difference network topology (MCI-NC), where the green edges denote those having statistically decreased ($p < 0.05$, Bonferroni correction) linkage.

($p < 0.005$) was observed. On the alpha2 network, significant effects of the referencing methods on the cluster coefficient (F (2, 36) = 3.611, $p < 0.045$) and the shortest path length (F (2, 36) = 4.739, $p < 0.028$) were observed, respectively. The interaction between Ref *group was also significant (the cluster coefficient: F (2, 36) = 6.036, $p < 0.008$; the shortest path length: F (2, 36) = 5.452, $p < 0.019$). The post hoc t-test (Bonferroni correction) revealed that significant differences on referencing methods occur (the cluster coefficient: AR versus VR, $p < 0.035$; the shortest path length: IR versus AR ($p < 0.028$), AR versus VR ($p < 0.023$)). In addition, significant effects between the groups (MCI versus normal) (all ps < 0.000) were observed. On the beta network, significant effects of the referencing methods on the cluster coefficient (F (2, 36) = 57.010, $p < 0.000$) and the shortest path length (F (2, 36) = 38.048, $p < 0.000$) were observed. The interactions between Ref *group were non-significant (all ps > 0.05). A post hoc t-test (Bonferroni adjusted) revealed that a significant difference on referencing methods occurs (the cluster coefficient between IR and VR ($p < 0.009$); the shortest path length between IR and VR and between AR and VR (all ps < 0.000)). On the gamma network, significant effects of the referencing methods on the cluster coefficient (F (2, 36) = 31.397, $p < 0.000$) and the shortest path length (F (2, 36) = 27.902, $p < 0.000$) were observed. The interaction between the Ref *group on the cluster coefficient was non-significant

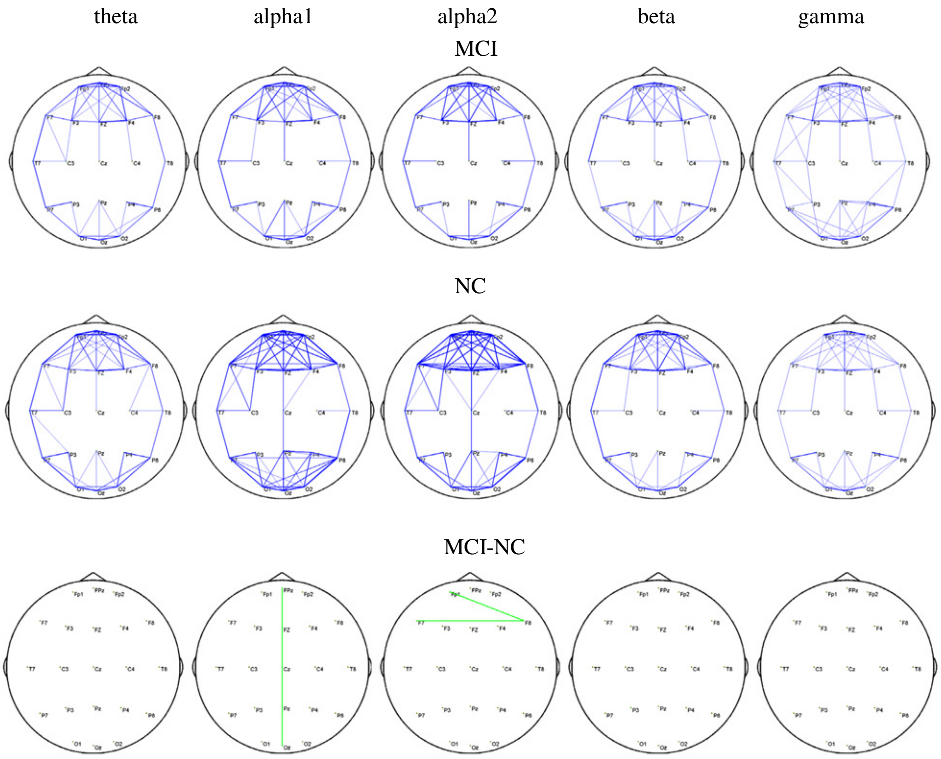

(b) VR

Figure 2. (Continued.)

(F (2, 36) = 1.602, $p < 0.216$). Post hoc t-test (Bonferroni correction) analysis revealed that the IR has a significant difference with both AR ($p < 0.055$, marginal significant) and VR ($p < 0.001$) on the cluster coefficient, respectively. It was also found that IR shows significant differences between other referencing methods (all ps < 0.05), and a significant difference was observed between AR and VR ($p < 0.001$) on the shortest path length. The significant statistical test ($p < 0.05$, Bonferroni correction) revealed that the network parameters of alpha1 and alpha2 could distinctly differentiate the MCI and NC groups.

3.3. ROC of the network parameters and mean coherence

Figure 4 shows the ROC of the clustering coefficients (C) for different EEG bands when the three references were adopted, separately. For the shortest path length (L) and MCoh, the ROC curves are similar and are therefore omitted here. Table 2 summarizes the AUCs of the three parameters (C, L, MCoh) for different EEG bands based on each of the three references. These results again indicate that the IR EEG-based parameters have a stronger differentiation ability for MCI recognition. Table 2 also clearly demonstrates that the network parameters (C, L) have more differentiating ability than does MCoh.

3.4. MCI recognition

Based on the results shown in figures 3–4 and table 2, the two network parameters and MCoh are strikingly different for the MCI and NC groups in alpha1 and alpha2; thus, they are

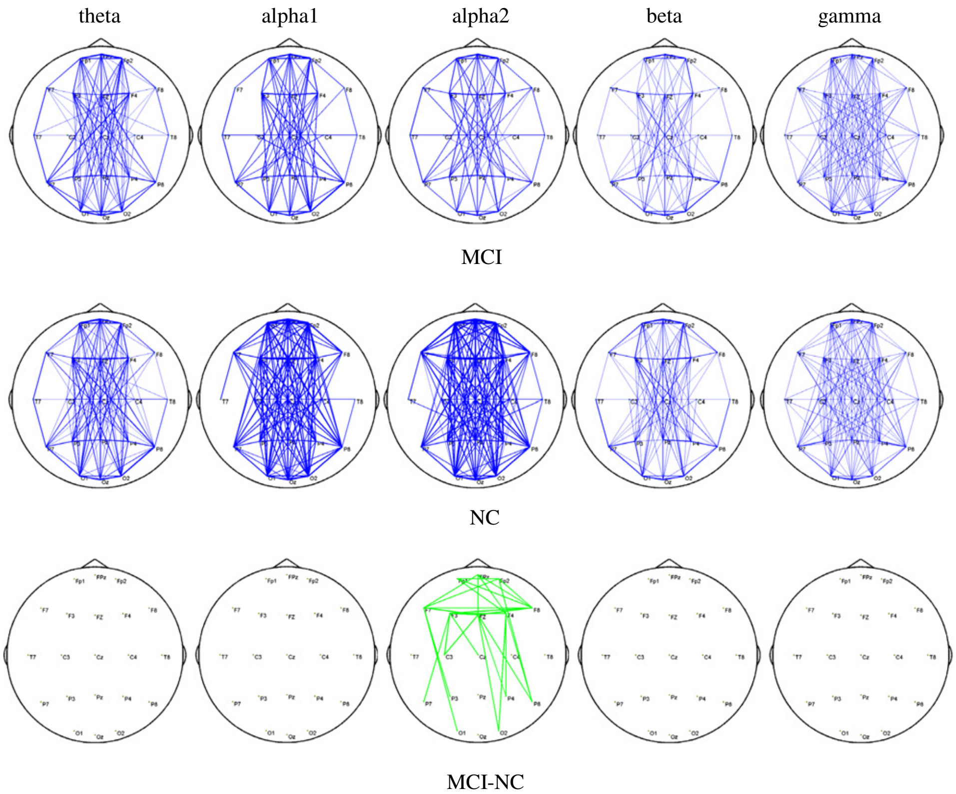

(c) AR

Figure 2. (Continued.)

considered to be the potential features for MCI recognition using LDA and SVM, respectively. Specifically, for the network based recognition, the feature is composed of the clustering coefficients (C) and the shortest path length (L), resulting in the two-dimensional feature for one concerned frequency band. As for the MCoh, the feature is of one dimension for one concerned frequency band. When the features in alpha1 and alpha2 bands are combined, the features in the separate band are simply connected to generate the double length features compared to that in the separate frequency band. Considering that the subject number was relatively small, the classification was performed using the leave-one-out strategy (Xu *et al* 2010a, Dauwels *et al* 2010a). Table 3 gives the classification Acc, Spe and Sen when different combinations of features under the three references are used for classification. The results also clearly indicate that the classifications based on the network parameters are usually much better than those that are based on traditional Coh. The parameters that are derived from IR and based on EEG perform better in classification than do those obtained from the other two non-zero references.

4. Discussion

4.1. The topology difference

Figure 2 revealed that the two groups exhibit different topologies, and the significant differences between the two groups all converged to the alpha1 and alpha2 bands for the three different

Table 2. The AUC for network properties and mean coherence under different reference choices in different EEG frequency bands.

	Theta			Alpha1			Alpha2			Beta			Gamma		
	C	*L*	MCoh	*C*	*L*	MCoh	*C*	*L*	MCoh	*C*	*L*	MCoh	*C*	*L*	MCoh
VR	0.62	0.60	0.65	**0.89**	**0.87**	**0.83**	0.86	0.89	0.93	0.62	0.61	0.60	**0.73**	**0.76**	**0.81**
AR	0.55	0.57	0.56	0.80	0.79	0.75	0.97	0.97	0.93	0.66	0.65	0.59	0.55	0.56	0.63
IR	**0.78**	**0.79**	**0.73**	**0.89**	**0.87**	**0.83**	**0.98**	**0.97**	**0.97**	**0.67**	**0.68**	**0.64**	0.58	0.59	0.65

* *C* is the clustering coefficient, *L* is the shortest path length, and MCoh is the mean coherence.
The bold digits indicate the largest AUC among the three references.

Table 3. The classification performance for MCI recognition.

		Alpha 1						Alpha 2						Alpha1+alpha 2					
		Acc (%)		Spe (%)		Sen (%)		Acc (%)		Spe (%)		Sen (%)		Acc (%)		Spe (%)		Sen (%)	
		NET	MCoh	NET	MCoh	NET	MCoh	NET	MCoh	NET	MCoh	NET	MCoh	NET	MCoh	NET	MCoh	NET	MCoh
LDA	VR	75	70	70	70	80	70	80	75	**90**	70	70	80	**90**	75	**100**	70	80	80
	AR	65	70	60	70	70	70	85	75	80	70	90	80	75	75	70	70	80	80
	IR	**85**	**80**	**80**	**80**	**90**	**80**	**90**	**85**	80	**80**	**100**	**90**	85	**80**	70	70	**100**	**90**
SVM	VR	75	70	70	**70**	**80**	70	75	75	**80**	70	70	80	65	70	60	60	70	**80**
	AR	75	65	70	50	**80**	**80**	80	70	70	60	90	80	75	65	70	50	80	**80**
	IR	**80**	**75**	**80**	**70**	**80**	**80**	**90**	**85**	**80**	**80**	**100**	**90**	**85**	**75**	**80**	**80**	**90**	70

VR = vertex reference; AR = average reference; IR = infinity zero reference; Acc = accuracy; Sen = sensitivity; Spe =s; NET = network properties; MCoh = mean coherence.
The bold digit indicates the best performance among the three references for the two classifiers, respectively.
Alpha1, alpha2 and alpha1+alpha2 denote that the corresponding network and coherence features in those frequency bands are separately used for MCI recognition.

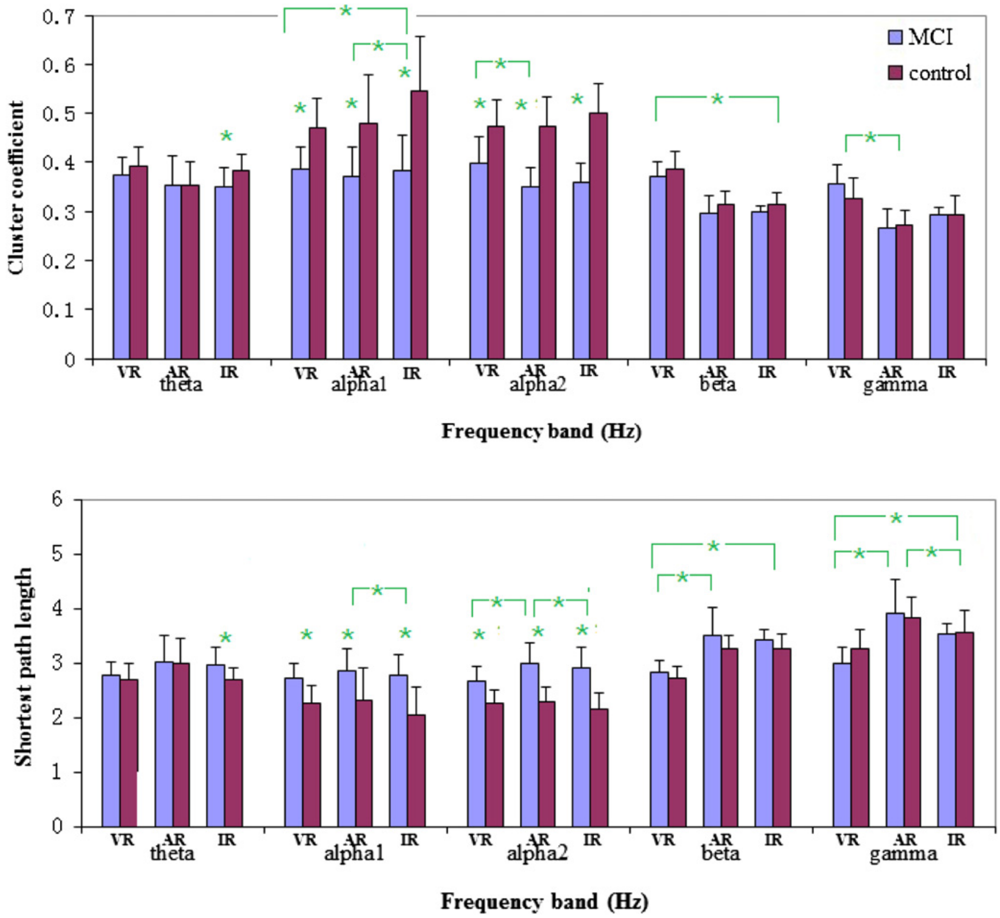

Figure 3. The parameter differences of the EEG networks with different references (VR, AR, IR). * indicates $p < 0.05$ (Bonferroni correction) between the MCI and control groups; –*– indicates $p < 0.05$ (Bonferroni correction) between the corresponding references.

references. Such an agreement in the results among different references strongly suggests that the differences between the two groups exist mainly in alpha1 and alpha2, and thus, the corresponding network features in these two bands could be reliable for discriminating these two groups. Based on these topology differences, MCI patients could have dramatically decreased linkages between the frontal and posterior areas in the alpha band, which indicates that MCI could be partly due to the weakened long-range linkage in the brain.

Figure 2 also showed that the detailed topologies that correspond to the three references had large differences. For example, VR-based EEG networks had less connection in the parietal area close to the vertex. In fact, when the VR is used, those electrodes that are close to the reference electrode naturally have similar EEG information as the reference channel, and therefore, useful information could be lost due to the subtraction of the EEG waveforms at the vertex. Compared to VR, both IR (REST) and AR can result in a meaningful network topology with abundant long-range connections between frontal and posterior areas. In our previous evaluations of REST (Qin *et al* 2010, Yao 2001, 2005), AR was proved to be the closest to

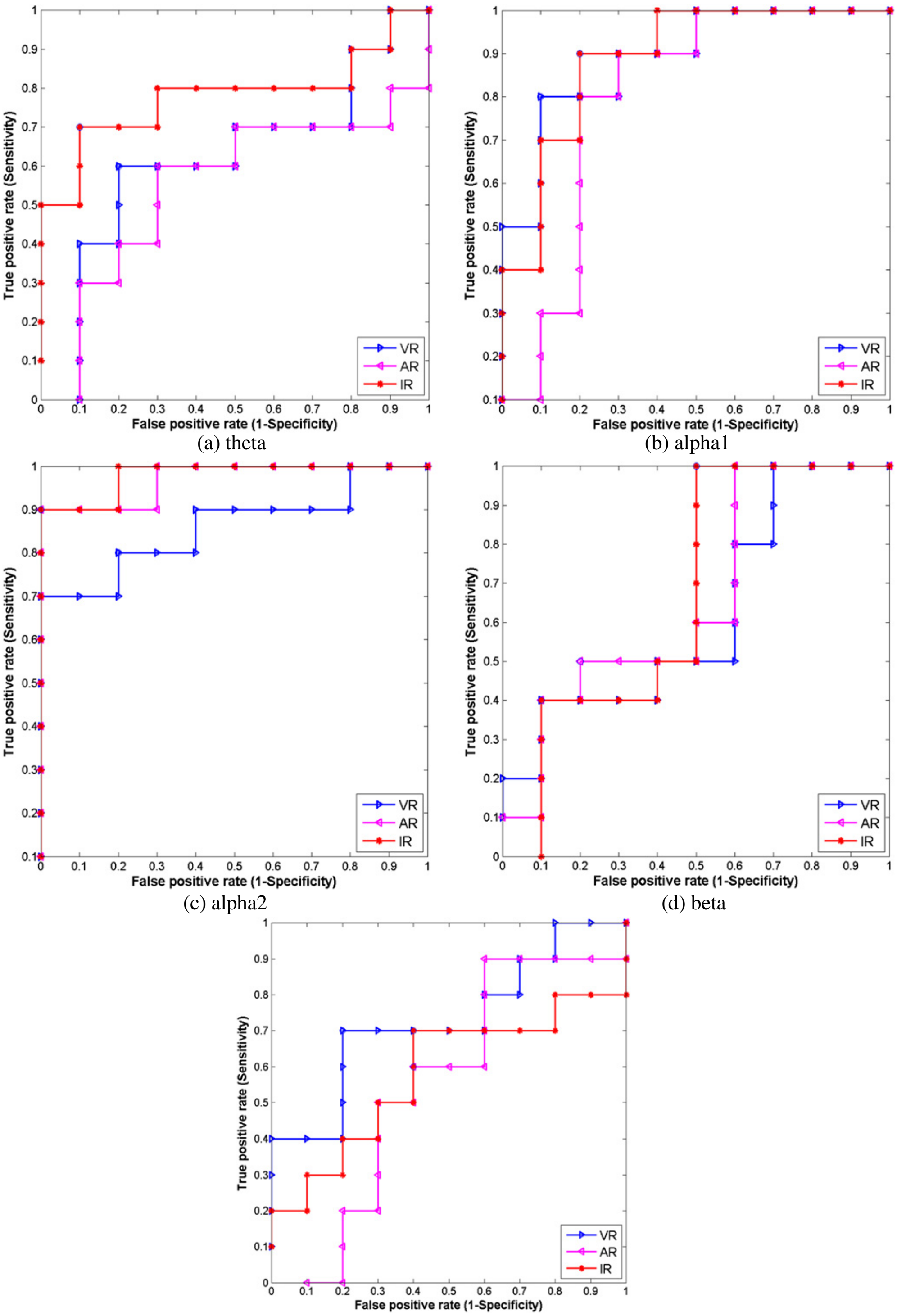

(a) theta

(b) alpha1

(c) alpha2

(d) beta

(e) gamma

Figure 4. The ROC of the clustering coefficients for the three references in different EEG frequency bands.

REST because the average of all of the electrodes would lower the dependence of the reference on any specific electrode (Thatcher 2012). More specifically, if an electrode configuration was sufficiently dense and covered the whole surface evenly, then AR would also be a true zero reference (Yao 2001).

4.2. The difference in the network parameters

As illustrated in figure 3, the network properties in alpha1 and alpha2 showed significant differences between the two groups regardless of the reference that was adopted. Specifically, the MCI group showed the decreased clustering coefficients and increased shortest path length compared to the control group, while no consistent and obvious differences were revealed in the other relevant EEG bands. The most obvious differences were revealed in the alpha band and are consistent with previous studies, which reported a decrease in the Coh in the alpha band for MCI and AD (Adler *et al* 2003, Locatelli *et al* 1998, Stam *et al* 2003). From a network perspective, the clustering coefficients and the shortest path length represent the processing ability of the brain for local and global information, respectively. The decreased clustering coefficients and increased shortest path length in alpha1 and alpha2 for MCI consistently demonstrated that MCI patients have less efficiency in processing both local and global information, which could account for cognition problems such as the memory impairment that is usually encountered by aMCI patients (Petersen *et al* 2001, Pijnenburg *et al* 2004, Portet *et al* 2006). Interestingly, VR shows the relatively obvious network parameter difference in the Gamma band. In van Deursen *et al* (2008), although increased Gamma activity has been revealed between MCI and the control under task conditions, no difference is observed in the resting state for the two groups. Based on this finding, we could further prove the important effect of the reference choice on the EEG analysis and that VR could result in a controversial difference between the two groups in the Gamma band.

Consistent with the topology difference revealed in figure 2, an obvious difference in network properties between the two groups still exists in alpha1 and alpha2 for the three references. However, the EEG reference choices actually have obvious effects on the concerned EEG properties ($p < 0.05$, Bonferroni correction). Figure 3 and the ANOVA test results show that IR can uncover differences most reliably in alpha1 and alpha2 with the smallest p-value compared to the other two references, and thus, it provides more chances to discern the MCI patients. In other words, transforming a traditional reference to the zero reference by REST could partially recover the lost information that is induced by the non-zero reference; therefore, this approach gives a higher likelihood of finding the truly existing differences between MCI and NC.

4.3. AUC of the network parameters and MCoh

To further confirm the feasibility of the network parameters for MCI recognition, the AUC of the network parameters (C, L) and MCoh were calculated and compared in the concerned EEG bands. According to table 2, three basic facts were clearly revealed: (a) the two network parameters have a higher discriminative ability than MCoh, which indicates that the network approach for MCI recognition is a better method than the previous MCoh-based approach; (b) the alpha1 and alpha2 bands are the two best bands for MCI classification because the AUC of these two bands are distinctly larger than the other bands, for either the network properties or MCoh, and thus, these two bands are adopted for MCI recognition in this work; and (c) regardless of which parameter is adopted, the EEG based on IR consistently provides the largest AUC for the concerned frequency bands except for gamma, which means that REST partially recovers the lost information that is induced by the non-zero reference. As mentioned in section 4.2, VR can contribute the controversial difference between the MCI and control group in the Gamma band, which could account for this exception.

4.4. The MCI recognition

Based on the most prominent AUCs that existed in alpha1 and alpha2, the network and MCoh features in those two bands were used for MCI recognition. Table 3 clearly shows the classification differences between the network properties and the MCoh. When the same reference was adopted, the network feature-based recognition outperformed the MCoh-based classification (with only one exception in the alpha1 band, when LDA is used for the AR reference features). The classification Acc using the MCoh is between ∼75% and ∼85%, which is consistent with the 78%–84% Acc based on the scalp EEG, as reported in previous studies (Bennys *et al* 2001, Buscema *et al* 2007, Cichocki *et al* 2005, Rossini *et al* 2008, Stam *et al* 2003). In the current work, the 90% Acc was achieved when the network features in the alpha2 band were adopted for MCI recognition. Unlike the MCI recognition studies that use the power spectrum or Coh, the current work used network properties as the basis for classification. MCI disorder has been proven to involve the abnormality of multiple brain areas just as the different network topology shown in figure 2. In essence, network properties are the statistical measurement of the spatial topology and it can capture the topology information for MCI recognition. Therefore, it may be more appropriate to explain and classify the MCI from the network perspective (Ding *et al* 2013, Rombouts *et al* 2005, Seo *et al* 2013).

Table 3 also demonstrated that the EEG reference choice did influence the MCI recognition, where the EEG with IR from REST could provide the higher recognition ability (>85%) for most of the tested cases, regardless of whether the different feature combinations or the different classifiers were adopted, compared to the other two non-zero references. More importantly, one critical criterion for a clinical application is to recognize the patients as accurately as possible; in other words, a high Sen that denotes less possibility of failing to recognize the MCI patients is expected. Table 3 showed that IR can reach a recognition Sen of above 90%, which is consistently much higher than the other two references for the two classifiers when the network features are considered.

In the current work, the NC group is screened using relatively strict criteria to select the NC subjects that have a high performance, which could result in reliable differentiation, as reported in the current work. However, among the different reference and metric-based classifications, recognition based on network properties constructed with a zero reference consistently has the best Acc in most of the concerned frequency bands. IR in the current work is realized using the 3-shell sphere head model, and the realistic head model constructed for a specific individual may further improve the closeness of the reference to the actual zero reference. A possible limitation of the current work is that the MCI dataset is relatively small. Although the results are stable and promising, more subjects are needed to further confirm the findings. Another possible solution to improve MCI recognition performance is to combine various types of features and use the feature selection criteria to choose the compensational information (Dauwels *et al* 2010a). Compared with other techniques like fMRI, EEG is usually non-stationary, which may influence the related analysis. The future study needs to pay special attention to this issue. In addition to the methodology development, a difficulty for the accurate diagnosis of MCI arises mainly because of the very limited knowledge about the underlying neural mechanism of MCI, and a more reliable recognition is dependent on future studies for the related neural mechanism (Albert *et al* 2011, Dauwels *et al* 2010a, Rossini *et al* 2008).

5. Conclusions

The conducted studies demonstrate that the resting network of the scalp EEG with a zero reference that is realized by REST can be used to robustly classify the MCI with an Acc of approximately 90%, which is close to the classification obtained using MRI (Fan *et al* 2008, Misra *et al* 2009, Wee *et al* 2012). Compared with the existing MCI classification studies that use EEG, the performance improvement of the current work can be attributed to the following exclusive techniques: (a) first of all, the network properties have more discriminative ability than the traditional Coh for the MCI recognition, possibly because the network view is a better portrayal of the intrinsic neural mechanisms of MCI; and (b) IR-based EEG data can construct networks to save information about the truly existing differences between MCI and NC; in other words, REST can partially recover the lost information that is caused by a non-zero transformation.

Acknowledgments

We declare that there is no conflict of interest for this work. This work was supported in part by grants from 973 program 2011CB707803, the National Nature Science Foundation of China (nos 61175117, 31070881 and 31100745), the program for New Century Excellent Talents in University (NCET-12-0089) and the 863 project 2012AA011601.

References

Adler G, Brassen S and Jajcevic A 2003 EEG coherence in Alzheimer's dementia *J. Neural Transm.* **110** 1051–8

Albert M S, DeKosky S T, Dickson D, Dubois B, Feldman H H, Fox N C, Gamst A, Holtzman D M, Jagust W J and Petersen R C 2011 The diagnosis of mild cognitive impairment due to Alzheimer's disease: recommendations from the national institute on aging-Alzheimer's association workgroups on diagnostic guidelines for Alzheimer's disease *Alzheimers Dement.* **7** 270–9

Babiloni C *et al* 2006 Fronto-parietal coupling of brain rhythms in mild cognitive impairment: a multicentric EEG study *Brain Res. Bull.* **69** 63–73

Bai F, Shu N, Yuan Y, Shi Y, Yu H, Wu D, Wang J, Xia M, He Y and Zhang Z 2012 Topologically convergent and divergent structural connectivity patterns between patients with remitted geriatric depression and amnestic mild cognitive impairment *J. Neurosci.* **32** 4307–18

Bai F, Watson D R, Yu H, Shi Y, Yuan Y and Zhang Z 2009 Abnormal resting-state functional connectivity of posterior cingulate cortex in amnestic type mild cognitive impairment *Brain Res.* **1302** 167–74

Bennys K, Rondouin G, Vergnes C and Touchon J 2001 Diagnostic value of quantitative EEG in Alzheimer's disease *Neurophysiol. Clin.* **31** 153–60

Bischkopf J, Busse A and Angermeyer M 2002 Mild cognitive impairment—a review of prevalence, incidence and outcome according to current approaches *Acta Psychiatr. Scand.* **106** 403–14

Brookmeyer R, Johnson E, Ziegler-Graham K and Arrighi H M 2007 Forecasting the global burden of Alzheimer's disease *Alzheimers Dement.* **3** 186–91

Buscema M, Rossini P, Babiloni C and Grossi E 2007 The IFAST model, a novel parallel nonlinear EEG analysis technique, distinguishes mild cognitive impairment and Alzheimer's disease patients with high degree of accuracy *Artifi. Intell. Med.* **40** 127–41

Chang C-C and Lin C-J 2011 LIBSVM: a library for support vector machines *ACM Trans. Intell. Syst. Technol.* **2** 27

Cichocki A, Shishkin S L, Musha T, Leonowicz Z, Asada T and Kurachi T 2005 EEG filtering based on blind source separation (BSS) for early detection of Alzheimer's disease *Clin. Neurophysiol.* **116** 729–37

Dauwels J, Srinivasan K, Reddy M R, Musha T, Vialatte F B, Latchoumane C, Jeong J and Cichocki A 2011 Slowing and loss of complexity in Alzheimer's EEG: two sides of the same coin *Int. J. Alzheimers Dis.* **2011** 539621

Dauwels J, Vialatte F and Cichocki A 2010a Diagnosis of Alzheimer's disease from EEG signals: where are we standing *Curr. Alzheimer. Res.* **7** 487–505

Dauwels J, Vialatte F, Musha T and Cichocki A 2010b A comparative study of synchrony measures for the early diagnosis of Alzheimer's disease based on EEG *Neuroimage* **49** 668–93

Dickerson B C *et al* 2004 Medial temporal lobe function and structure in mild cognitive impairment *Ann. Neurol.* **56** 27–35

Ding J R *et al* 2013 Altered functional and structural connectivity networks in psychogenic non-epileptic seizures *PLoS One* **8** e63850

Fan Y, Batmanghelich N, Clark C M and Davatzikos C 2008 Spatial patterns of brain atrophy in MCI patients, identified via high-dimensional pattern classification, predict subsequent cognitive decline *Neuroimage* **39** 1731

Ferri C P *et al* 2005 Global prevalence of dementia: a Delphi consensus study *Lancet* **366** 2112–7

Geselowitz D B 1998 The zero of potential *IEEE Eng. Med. Biol. Mag.* **17** 128–36

Gomez C, Stam C J, Hornero R, Fernandez A and Maestu F 2009 Disturbed beta band functional connectivity in patients with mild cognitive impairment: an MEG study *IEEE Trans. Biomed. Eng.* **56** 1683–90

Grundman M, Petersen R C, Ferris S H, Thomas R G, Aisen P S, Bennett D A, Foster N L, Jack C R Jr, Galasko D R and Doody R 2004 Mild cognitive impairment can be distinguished from Alzheimer disease and normal aging for clinical trials *Arch. Neurol.* **61** 59

Huang C, Wahlund L O, Dierks T, Julin P, Winblad B and Jelic V 2000 Discrimination of Alzheimer's disease and mild cognitive impairment by equivalent EEG sources: a cross-sectional and longitudinal study *Clin. Neurophysiol.* **111** 1961–7

Jeong J 2004 EEG dynamics in patients with Alzheimer's disease *Clin. Neurophysiol.* **115** 1490–505

Koenig T, Prichep L, Dierks T, Hubl D, Wahlund L O, John E R and Jelic V 2005 Decreased EEG synchronization in Alzheimer's disease and mild cognitive impairment *Neurobiol. Aging* **26** 165–71

Koopmans L H 1995 *The Spectral Analysis of Time Series (Probability and Mathematical Statistics* vol 22*)* (New York: Academic)

Locatelli T, Cursi M, Liberati D, Franceschi M and Comi G 1998 EEG coherence in Alzheimer's disease *Electroencephalogr. Clin. Neurophysiol.* **106** 229–37

Marzetti L, Nolte G, Perrucci M, Romani G and Del Gratta C 2007 The use of standardized infinity reference in EEG coherency studies *Neuroimage* **36** 48–63

Misra C, Fan Y and Davatzikos C 2009 Baseline and longitudinal patterns of brain atrophy in MCI patients, and their use in prediction of short-term conversion to AD: results from ADNI *Neuroimage* **44** 1415

Nunez P L, Silberstein R B, Shi Z, Carpenter M R, Srinivasan R, Tucker D M, Doran S M, Cadusch P J and Wijesinghe R S 1999 EEG coherency: II. Experimental comparisons of multiple measures *Clin. Neurophysiol.* **110** 469–86

Petersen R C, Doody R, Kurz A, Mohs R C, Morris J C, Rabins P V, Ritchie K, Rossor M, Thal L and Winblad B 2001 Current concepts in mild cognitive impairment *Arch. Neurol.* **58** 1985

Petersen R C, Smith G E, Ivnik R J, Tangalos E G, Schaid D J, Thibodeau S N, Kokmen E, Waring S C and Kurland L T 1995 Apolipoprotein E status as a predictor of the development of Alzheimer's disease in memory-impaired individuals *J. Am. Med. Assoc.* **273** 1274–8

Petrosian A, Prokhorov D, Lajara-Nanson W and Schiffer R 2001 Recurrent neural network-based approach for early recognition of Alzheimer's disease in EEG *Clin. Neurophysiol.* **112** 1378–87

Pijnenburg Y A, van der Made Y, van Cappellen van Walsum A M, Knol D L, Scheltens P and Stam C J 2004 EEG synchronization likelihood in mild cognitive impairment and Alzheimer's disease during a working memory task *Clin. Neurophysiol.* **115** 1332–9

Portet F, Ousset P J, Visser P J, Frisoni G B, Nobili F, Scheltens P, Vellas B and Touchon J 2006 Mild cognitive impairment (MCI) in medical practice: a critical review of the concept and new diagnostic procedure. Report of the MCI working group of the European consortium on Alzheimer's disease *J. Neurol. Neurosurg. Psychiatry* **77** 714–8

Qin Y, Xu P and Yao D 2010 A comparative study of different references for EEG default mode network: the use of the infinity reference *Clin. Neurophysiol.* **121** 1981–91

Rombouts S A, Barkhof F, Goekoop R, Stam C J and Scheltens P 2005 Altered resting state networks in mild cognitive impairment and mild Alzheimer's disease: an fMRI study *Hum Brain Mapp.* **26** 231–9

Rossini P M, Buscema M, Capriotti M, Grossi E, Rodriguez G, Del Percio C and Babiloni C 2008 Is it possible to automatically distinguish resting EEG data of normal elderly versus mild cognitive impairment subjects with high degree of accuracy? *Clin. Neurophysiol.* **119** 1534–45

Seo E H, Lee D Y, Lee J M, Park J S, Sohn B K, Lee D S, Choe Y M and Woo J I 2013 Whole-brain functional networks in cognitively normal, mild cognitive impairment, and Alzheimer's disease *PLoS One* **8** e53922

Stam C, De Haan W, Daffertshofer A, Jones B, Manshanden I, van Walsum A M C, Montez T, Verbunt J, De Munck J and Van Dijk B 2009 Graph theoretical analysis of magnetoencephalographic functional connectivity in Alzheimer's disease *Brain* **132** 213–24

Stam C J, van der Made Y, Pijnenburg Y A and Scheltens P 2003 EEG synchronization in mild cognitive impairment and Alzheimer's disease *Acta Neurol. Scand.* **108** 90–6

Thatcher R W 2012 Coherence, phase differences, phase shift, and phase lock in EEG/ERP analyses *Dev. Neuropsychol.* **37** 476–96

van Deursen J A, Vuurman E F, Verhey F R, van Kranen-Mastenbroek V H and Riedel W J 2008 Increased EEG gamma band activity in Alzheimer's disease and mild cognitive impairment *J. Neural Transm.* **115** 1301–11

Wee C, Yap P, Zhang D, Denny K, Browndyke J, Potter G, Welsh-Bohmer K, Wang L and Shen D 2012 Identification of MCI individuals using structural and functional connectivity networks *Neuroimage* **59** 2045

Xu P, Kasprowicz M, Bergsneider M and Hu X 2010a Improved noninvasive intracranial pressure assessment with nonlinear kernel regression *IEEE Trans. Inf. Technol. Biomed.* **14** 971–8

Xu P, Tian Y, Chen H and Yao D 2007 Lp norm iterative sparse solution for EEG source Localization *IEEE Trans. Biomed. Eng.* **54** 400–9

Xu P, Tian Y, Lei X and Yao D 2010b Neuroelectric source imaging using 3SCO: a space coding algorithm based on particle swarm optimization and l0 norm constraint *Neuroimage* **51** 183–205

Yao D 2001 A method to standardize a reference of scalp EEG recordings to a point at infinity *Physiol. Meas.* **22** 693

Yao D, Wang L, Oostenveld R, Nielsen K D, Arendt-Nielsen L and Chen A C N 2005 A comparative study of different references for EEG spectral mapping: the issue of the neutral reference and the use of the infinity reference *Physiol. Meas.* **26** 173